Neuron
Article

Closing the Gate in the Limbic Striatum: Prefrontal Suppression of Hippocampal and Thalamic Inputs

Gwendolyn G. Calhoon[1,2] and Patricio O'Donnell[1,2,3,*]
[1]Program in Neuroscience
[2]Department of Anatomy & Neurobiology
[3]Department of Psychiatry
University of Maryland School of Medicine, Baltimore, MD 21201, USA
*Correspondence: podon002@umaryland.edu
http://dx.doi.org/10.1016/j.neuron.2013.01.032

SUMMARY

Many brain circuits control behavior by integrating information arising from separate inputs onto a common target neuron. Neurons in the ventral striatum (VS) receive converging excitatory afferents from the prefrontal cortex (PFC), hippocampus (HP), and thalamus, among other structures, and the integration of these inputs is critical for goal-directed behaviors. Although HP inputs have been described as gating PFC throughput in the VS, recent data reveal that the VS desynchronizes from the HP during epochs of burst-like PFC activity related to decision making. It is therefore possible that PFC inputs locally attenuate responses to other glutamatergic inputs to the VS. Here, we found that delivering trains of stimuli to the PFC suppresses HP- and thalamus-evoked synaptic responses in the VS, in part through activation of inhibitory processes. This interaction may enable the PFC to exert influence on basal ganglia loops during decision-making instances with minimal disturbance from ongoing contextual inputs.

INTRODUCTION

The ventral striatum (VS) has been described as the "limbic-motor interface" because it is strategically poised to integrate emotional-motivational input and subsequently influence motor activity (Mogenson et al., 1980). The VS encompasses the nucleus accumbens and ventromedial aspects of the dorsal striatum, as defined by the territories innervated by limbic inputs arriving from the hippocampus (HP) and medial prefrontal cortex (PFC) (Voorn et al., 2004), and integrates these and other afferent inputs to guide behavior. Individual medium spiny neurons (MSNs) of the VS receive afferents from the HP on proximal dendrites (Meredith et al., 1990), as well as the amygdala, thalamus, and PFC, in their more distal arbors (French and Totterdell, 2002, 2003; Moss and Bolam, 2008). VS MSNs must reconcile diverse and dynamic inputs into a cohesive efferent signal, and data suggest these inputs may interact in nonlinear ways (Goto and O'Donnell, 2002; O'Donnell and Grace, 1995). For example, HP inputs can drive VS MSNs into a depolarized up state, gating other inputs to the region (O'Donnell and Grace, 1995). This type of additive nonlinear interaction has been proposed to underlie the use of contextual information to guide motor plans.

During goal-directed behaviors and in decision-making instances, however, interactions among inputs to the VS may assume a different profile. PFC neurons fire in bursts during instrumental behavior (Chafee and Goldman-Rakic, 1998; Peters et al., 2005), and decision-making epochs are characterized by high-frequency oscillations in the gamma range (30–50 Hz). Robust, burst-like activation of the PFC reliably produces up states in VS MSNs (Gruber and O'Donnell, 2009). Furthermore, during behavioral epochs marked by high-frequency oscillations and burst firing in the PFC, the synchrony typically observed between the VS and the HP as coherent theta oscillations is lost in favor of a period of VS entrainment to the PFC (Gruber et al., 2009a). These findings suggest that the PFC is capable of disengaging the VS from the HP; thus, one excitatory projection can somewhat paradoxically reduce the efficacy of another glutamatergic input in VS MSNs.

Although input integration is typically additive for excitatory projections, competition among converging inputs can also occur. For example, in hippocampal slices, one set of inputs to CA1 neurons may reduce the efficacy of another (Alger et al., 1978; Lynch et al., 1977), and in the PFC, similar interactions between cortical and thalamic inputs have been reported (Fuentealba et al., 2004). Here, we tested whether brief, robust PFC activation disengages the VS from ongoing HP activity by way of heterosynaptic suppression in VS MSNs using in vivo intracellular recordings.

RESULTS

We performed in vivo intracellular recordings in 47 neurons from 36 adult male rats using standard recording conditions and 22 neurons from 15 rats using electrodes containing the $GABA_A$ antagonist picrotoxin. A subset of these cells (n = 10) were processed for Neurobiotin labeling and were morphologically identified as MSNs (Figure 1A). All neurons included in this study were

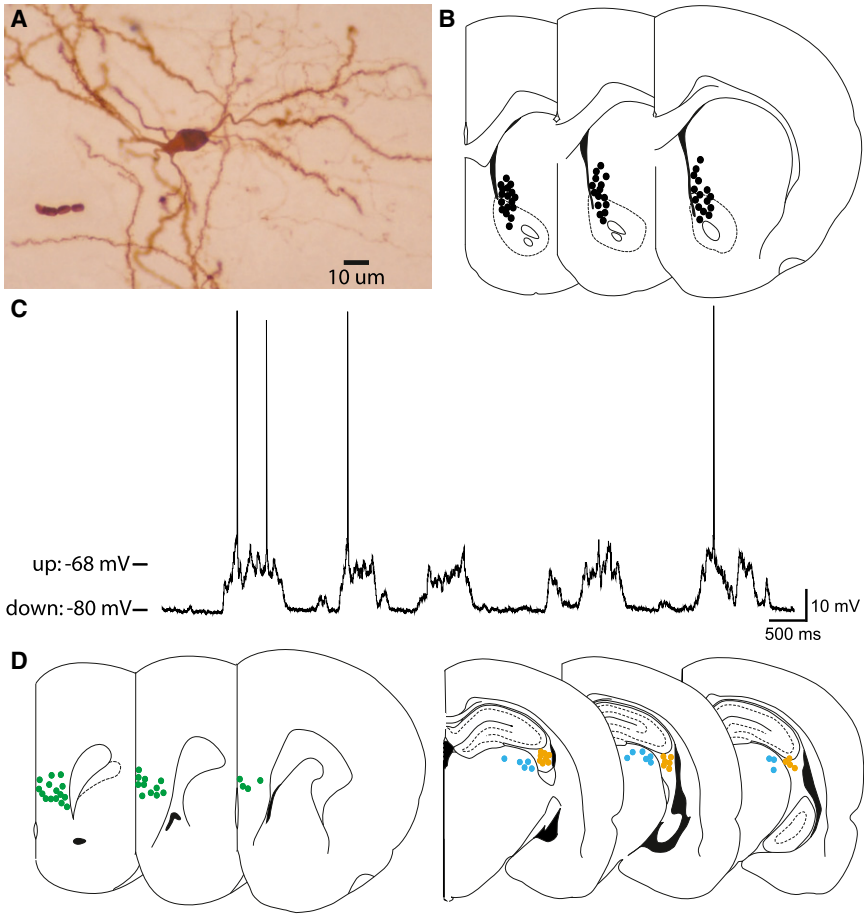

Figure 1. Intracellular Recordings of Medium Spiny Neurons In Vivo

(A) Image of an MSN filled with Neurobiotin and visualized with a diaminobenzidine reaction.

(B) Illustration of recording sites in the VS (dots represent cell locations). Recorded cells fell within the nucleus accumbens core, as well as dorsal to the classical nucleus accumbens boundaries, but within the region receiving afferents from the PFC and HP (Voorn et al., 2004).

(C) Representative trace showing spontaneous membrane potential of an MSN with transitions between a resting (down) state and the more depolarized up state at a frequency of 0.7 Hz. Action potentials originate exclusively from the up state.

(D) Illustration showing the location of stimulating electrode tips in the medial PFC (left, green, including both prelimbic and infralimbic regions), fimbria (right, orange), and dorsolateral thalamus (right, blue).

located within the striatal region receiving afferents from the medial PFC and HP (Voorn et al., 2004), including the nucleus accumbens core and the ventral aspect of the dorsomedial striatum (Figure 1B). All recorded cells exhibited spontaneous transitions between negative resting membrane potentials (down states; −84.1 ± 8.1 mV, mean ± SD) and depolarized up states (−70.9 ± 7.2 mV) closer to action potential threshold (Figure 1C). Up states occurred at a frequency of 0.6 ± 0.2 Hz with a duration of 521.8 ± 180.8 ms. The majority of recorded neurons were silent (29/47; 62%), but spontaneous firing was detected in the remaining 18 neurons at 0.96 ± 1.4 Hz (range, 0.01–5.2 Hz). Action potentials (spontaneous or evoked) in all neurons had an amplitude of 52.8 ± 7.9 mV from threshold. Input resistance in the down state was 54.5 ± 17.4 MΩ. These properties are similar to what has been previously reported in VS MSNs (Brady and O'Donnell, 2004; Goto and O'Donnell, 2001a, 2001b; O'Donnell and Grace, 1995).

High-Frequency PFC Stimulation Suppresses Fimbria-Evoked Synaptic Responses in MSNs

To assess whether robust PFC activation suppresses MSN responses to HP afferents, stimulating electrodes were targeted to the medial PFC and the fimbria-fornix, the fiber bundle carrying HP inputs to the VS (n = 21 neurons; Figure 1D). Single-pulse fimbria stimulation evoked excitatory postsynaptic potentials (EPSPs) with a mean amplitude of 7.6 ± 5.3 mV and time to peak of 36.1 ± 16.3 ms. Consistent with previous results (Gruber and O'Donnell, 2009), ten-pulse, 50 Hz train stimulation of the PFC elicited a prolonged depolarization but rarely action potentials in VS MSNs (Figure 2A). Only 4 of 27 MSNs responded with action potential firing during the PFC train stimulation; the majority remained silent during the PFC-evoked depolarization. We evaluated MSN responses to fimbria stimulation before and following PFC burst stimulation. At a short, 50 ms latency following the final pulse in the PFC train stimulus, the amplitude of the fimbria-evoked EPSP (F2) was 1.7 ± 2.0 mV, a value significantly reduced compared to the fimbria-evoked EPSP recorded 500 ms prior to PFC stimulation (F1) ($t_{(13)}$ = 5.679; $p < 0.0001$; Figure 2A), without affecting time to peak. HP afferent stimulation 500 ms after the last pulse in the PFC train did not show a suppression relative to the F1 response ($t_{(11)} = 1.462$; $p = 0.17$; Figure 2B). These data indicate that strong PFC activation similar to what is observed during instrumental behavior in awake animals transiently attenuates synaptic responses to HP afferents in VS MSNs.

Because PFC train stimulation evoked a sustained depolarization in MSNs, it is possible that the attenuation observed in F2 EPSPs resulted from the depolarization itself; the membrane potential may have neared the reversal potential of the fimbria-evoked response following the PFC stimulation. To evaluate this possibility, we assessed F1 and F2 EPSP magnitudes evoked at similar membrane potentials. We achieved these conditions either by considering F1 EPSPs evoked during spontaneous up states (eight neurons) or by injecting depolarizing current into the recorded cells through the recording electrode (four neurons). We tailored the amount of current injected for each cell to adjust the membrane potential to values similar to those evoked by the PFC train. When we compared F1 and F2

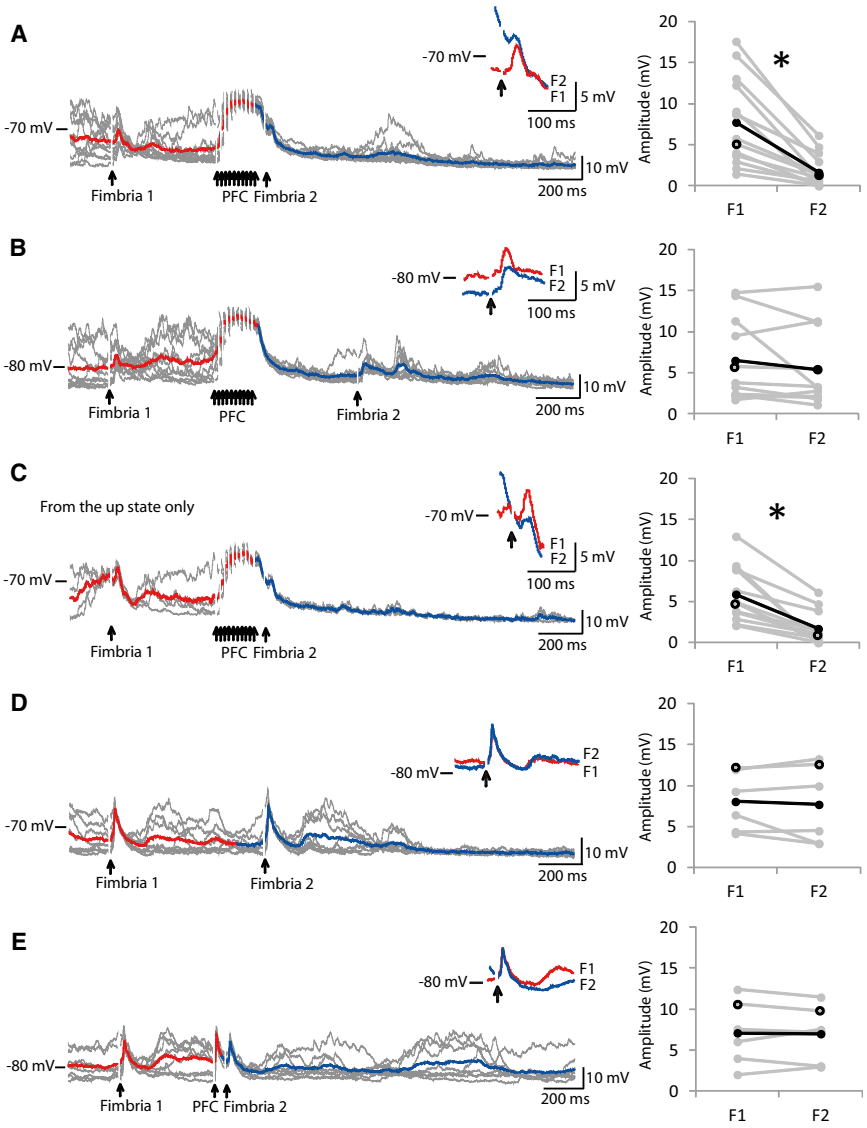

Figure 2. PFC High-Frequency Stimulation Inhibits Fimbria-Evoked EPSPs in MSNs at Short, but Not Long, Latencies

(A) Multiple overlaid sweeps showing a VS neuron's response to combined stimulation of PFC and HP inputs. An initial control pulse to the fimbria (F1) was followed by a train of 10 pulses (50 Hz) to the PFC and a test pulse to the fimbria (F2) 50 ms following the PFC train. Mean responses to F1 and F2 are highlighted in red and blue, respectively, and the initial 100 ms of both responses are shown as an inset. Right: Actual amplitude values of all F1 and F2 evoked responses are shown in gray (example traces indicated in open black circles in this and subsequent figures), whereas average values are shown in closed black, revealing a significant attenuation of F2 (*$p < 0.0001$; paired t test).

(B) Similar display illustrating responses obtained when F2 was delivered 500 ms following the PFC train stimulus in the same cell shown in (A). Mean responses to F1 and F2 are again shown as an inset, and plots to the right illustrate all F1 and F2 values obtained from this protocol, which did not significantly differ.

(C) Overlay of traces and their average recorded using the same protocol as in (A) but considering only traces in which F1 occurred during spontaneous up states. Up-state-evoked depolarization did not significantly reduce the amplitude of the response to the control fimbria stimulus. Right: Actual amplitude values of all depolarized F1 and basal F2 responses (gray) and their average (black), revealing an attenuation of F2. (*$p < 0.0003$; two-tailed paired t test).

(D) Overlay of responses to F1 and F2 stimulation without the intervening PFC train stimulation. Mean responses to F1 and F2 are highlighted in red and blue, respectively, and overlaid in the inset. Right: Plot of all F1 and F2 values obtained in these conditions showing absence of a significant difference.

(E) Overlay of traces showing F1 and F2 responses with single-pulse PFC stimulation in the same cell shown in (D). MSNs responded with an EPSP to single-pulse PFC stimulation, which did not significantly impact the F2 response. Inset shows overlay of average F1 (red) and F2 (blue) responses. Right: F1 and F2 amplitudes show absence of F2 attenuation 50 ms after a single PFC pulse.

EPSPs recorded at similar membrane potentials, the amplitude of the F2 EPSP evoked 50 ms after the PFC train was still attenuated relative to that of the depolarized F1 EPSP ($t_{(11)} = 5.304$; $p < 0.0003$; Figure 2C). These data suggest that depolarization-induced changes in ionic conductances are not responsible for the PFC-evoked attenuation of the F2 EPSP.

Stimulating HP afferents twice within a few hundred milliseconds could suppress the second response independently of any effect of the intervening PFC stimulation. To address this possibility, we omitted the PFC train from the stimulus protocol in a subset of neurons (n = 6). In these cases, we found no difference in EPSP amplitude between the F1- and F2-evoked responses ($t_{(5)} = 0.506$; $p = 0.635$; Figure 2D). Furthermore, a single-pulse PFC stimulus did not reduce the amplitude of the F2 EPSP evoked 50 ms after the PFC pulse ($t_{(5)} = 0.266$; $p = 0.80$; Figure 2E). The attenuation of HP inputs following PFC stimulation required a burst of stimuli, suggesting this type of interaction among inputs may occur only during behavioral conditions in which the PFC is strongly activated.

Specificity of Heterosynaptic Suppression in MSNs

To assess whether PFC-evoked suppression of HP responses can be generalized to other inputs, we tested the effects of PFC train stimulation on MSN responses to thalamic afferent activation. The thalamus is an important source of glutamatergic afferents to the VS (Berendse and Groenewegen, 1990), which may also play a role in behavioral responses. Single-pulse thalamus stimulation evoked a 6.0 ± 2.6 mV EPSP with a

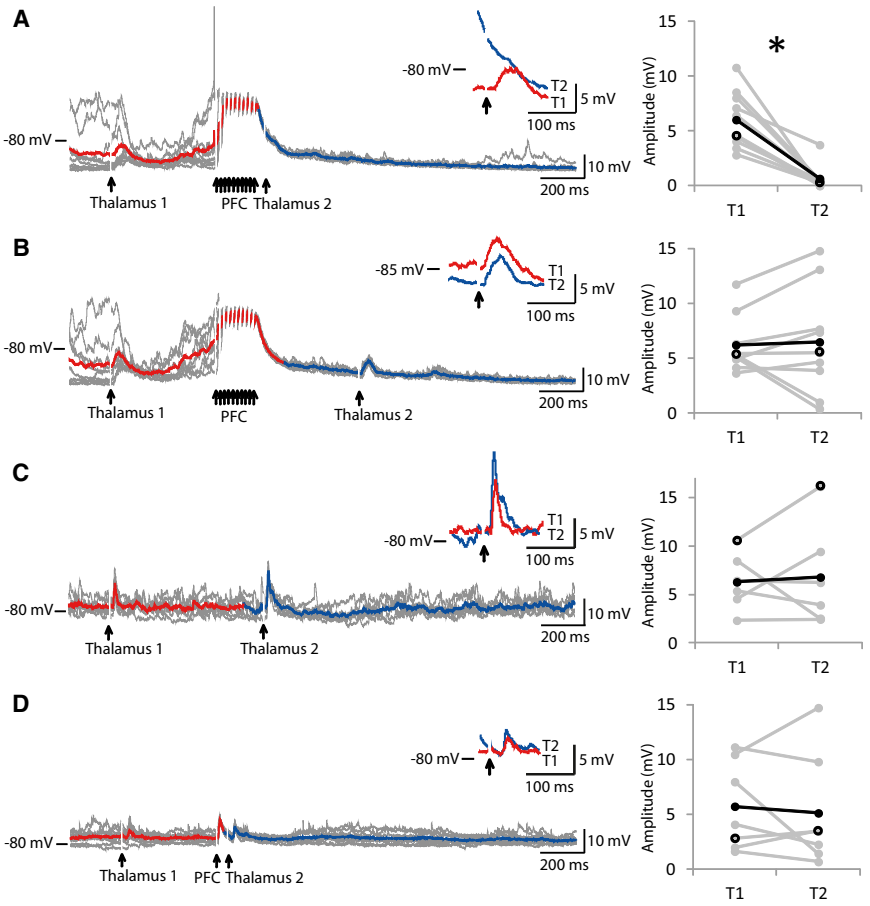

Figure 3. High-Frequency PFC Stimulation Suppresses Thalamus-Evoked Responses at Short, but Not Long, Latencies

(A) Average EPSPs evoked in a VS MSN by thalamus stimulation before (T1, red) and 50 ms after a ten-pulse, 50 Hz PFC train (T2, blue). An action potential that occurred immediately prior to the PFC stimulus train in one sweep is truncated. Right: Plot of T1 and T2 amplitudes (gray: all neurons; closed black: average) showing a significant reduction following PFC train stimulation (*$p < 0.0002$, paired t test).

(B) In the same cell shown in (A), the mean T2 (blue) amplitude is similar to T1 (red) 500 ms following the PFC train. Right: T1 and T2 values showing no difference.

(C) Average T1 (red) and T2 (blue) responses evoked in an MSN when no PFC stimulus was delivered. Right: Actual T1 and T2 values showing absence of attenuation.

(D) Average T1 (red) and T2 (blue) responses obtained from an MSN before and after single-pulse PFC stimulation. Right: Plot of T1 and T2 amplitudes illustrating the absence of F2 response attenuation by single-PFC pulses.

45.0 ± 17.8 ms time to peak. The amplitude of the thalamus-evoked EPSP was reduced to 0.7 ± 1.1 mV 50 ms following the last pulse in the PFC train ($t_{(9)} = 6.34$; $p < 0.0002$; $n = 10$; Figure 3A), but not 500 ms following the PFC train ($t_{(8)} = -0.27$; $p = 0.80$; Figure 3B). As was the case with fimbria-evoked responses, this suppression did not occur when the PFC train was omitted ($t_{(5)} = -0.29$; $p = 0.79$; Figure 3C) and could not be achieved using a single-pulse stimulus of the PFC ($t_{(6)} = 0.48$; $p = 0.65$; Figure 3D). The suppression of the thalamus-evoked response was not due to the PFC-elicited depolarization, as the amplitude of the EPSP evoked by the second thalamic stimulation (T2) remained significantly attenuated compared with the thalamus-evoked EPSP recorded prior to PFC stimulation (T1) at depolarized membrane potentials ($t_{(4)} = 2.76$; $p = 0.05$). These data suggest that strong PFC activation can elicit heterosynaptic suppression of multiple excitatory inputs to the VS.

To address whether heterosynaptic suppression in VS MSNs is an exclusive feature of strongly activated PFC inputs, we investigated whether PFC responses can in turn be subject to heterosynaptic suppression by strong activation of other glutamatergic inputs to the VS. We tested the impact of fimbria or thalamus train stimulation on EPSPs evoked by single-pulse PFC stimulation. Single-pulse PFC stimulation resulted in 11.3 ± 7.3 mV EPSPs in VS MSNs, with 18.3 ± 4.5 ms time to peak. A ten-pulse, 50 Hz train stimulation of the fimbria failed to suppress PFC-evoked responses 50 ms after the final pulse in the fimbria train ($t_{(5)} = 0.41$; $p = 0.70$; Figure 4A). The same train delivered to the thalamus, however, reduced the amplitude of the PFC-evoked EPSP to 7.5 ± 6.7 mV ($t_{(6)} = 3.8$; $p < 0.01$; Figure 4B) without affecting the time to peak. The magnitude of suppression elicited by thalamus stimulation was much less than that elicited by PFC stimulation. Burst-like PFC stimulation reduced the amplitude of the fimbria-evoked response by 81.3% ± 15.4% and reduced the amplitude of the thalamus-evoked response by 89.0% ± 15.2%, whereas high-frequency thalamus stimulation only reduced the PFC-evoked response by 37.0% ± 30.6%. In summary, PFC burst firing strongly attenuates HP and thalamic responses, strong thalamic activation has a moderate effect on PFC responses, and similarly strong activation of HP afferents does not diminish PFC responses. These data suggest that some, but not all, glutamatergic inputs to the VS affect responses evoked by other inputs by way of heterosynaptic suppression.

$GABA_A$ Receptors Contribute to Heterosynaptic Suppression in MSNs

As burst PFC stimulation activates VS local inhibitory processes (Gruber et al., 2009b), it is possible that local GABA neurotransmission contributes to the heterosynaptic suppression we report here. To assess this possibility, we included 200 μM picrotoxin in the intracellular solution for 22 cells from 15 adult male rats. As an open-channel blocker at the $GABA_A$ receptor, picrotoxin can antagonize $GABA_A$ signaling when applied outside or inside the cell membrane (Akaike et al., 1985; Cupello et al., 1991;

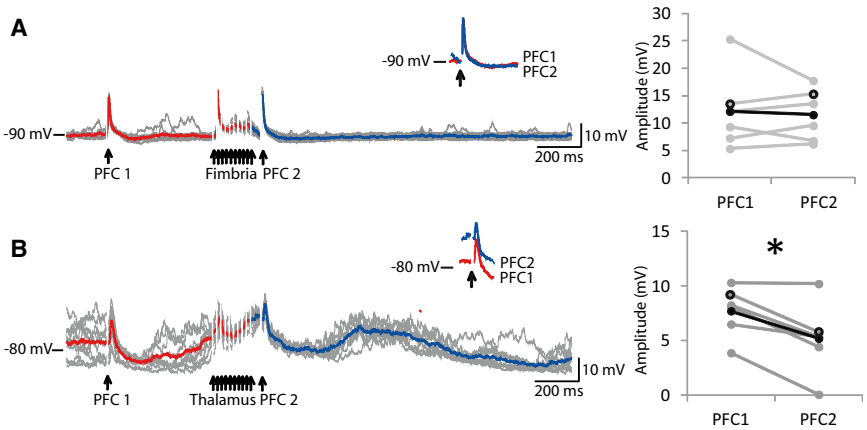

Figure 4. Effects of High-Frequency Stimulation of the Fimbria or Thalamus on PFC-Evoked Responses in VS MSNs

(A) Overlay of traces showing PFC-evoked EPSPs before (PFC 1) and 50 ms after (PFC 2) stimulation of HP afferents with a 50 Hz, ten-pulse train. Inset shows mean PFC 1 (red) and PFC 2 (blue) responses. Right: Plot of actual PFC1 and PFC2 values (gray) and their average (closed black) showing lack of modulation by the fimbria train.

(B) Overlay of traces showing PFC1 and PFC2 evoked responses before and 50 ms after a train of stimuli to the thalamus (ten pulses at 50 Hz), with the average responses shown in the inset. The plot to the right illustrates a significant suppression of PFC-evoked EPSPs in MSNs following strong thalamic activation (*$p < 0.01$, paired t test).

Inomata et al., 1988; Metherate and Ashe, 1993). We found that the presence of picrotoxin in the recording pipette impacted the baseline properties of recorded MSNs. MSNs treated with picrotoxin had similar resting potentials (−84.8 ± 7.6 mV), up-state frequency (0.7 ± 0.2 Hz), and up-state duration (470.8 ± 105.9 ms) to untreated cells. The up-state amplitude, however, was altered by the presence of picrotoxin (−66.6 ± 6.8 mV; $t_{(67)} = 2.7$; $p < 0.01$). Furthermore, the proportion of silent MSNs was reduced following picrotoxin treatment (7/22, 32%), and the spontaneous firing rate of active cells was enhanced relative to untreated cells (3.5 ± 3.5 Hz, range, 0.02–10.6 Hz; $t_{(31)} = 2.8$; $p < 0.01$; Figure 5A). This increase in baseline firing activity suggests that picrotoxin relieved some tonic inhibition normally exerted onto VS MSNs.

To assess whether $GABA_A$ antagonism reduced the PFC-driven suppression of the fimbria-evoked EPSP, we subjected picrotoxin-treated cells to the stimulation protocol described above. Picrotoxin did not significantly alter the F1-evoked EPSP, which had an amplitude of 8.5 ± 6.4 mV and a time to peak of 28.8 ± 6.9 ms. In the presence of picrotoxin, PFC train stimulation evoked sustained depolarizations similar to those elicited by the train in the absence of picrotoxin; however, a greater percentage of MSNs fired action potentials during the PFC train (6/12; 50%). Following picrotoxin administration, the amplitude of the F2-evoked response 50 ms after the PFC train was still reduced relative to that of the F1-evoked response ($t_{(11)} = 2.4$; $p < 0.05$; Figures 5C and 5D). Although this difference appeared to be driven by one cell in particular, the amplitude of the F1 response in this cell was not identified as an outlier by the fourth spread test (Hoaglin et al., 1983), so we included it in the analysis. However, the magnitude of PFC-evoked heterosynaptic suppression differed following PTX administration compared to the magnitude of suppression under baseline conditions. The PFC train reduced F2-evoked responses by 81.3% ± 15.4% in the absence of picrotoxin, whereas in the presence of picrotoxin, the magnitude of suppression was reduced to 49.6% ± 52.2%. The median magnitudes of suppression without and with PTX were 75.9% and 67.8%, respectively; the distributions in the two groups differed significantly (Mann-Whitney $U = 128$, $n_1 = 14$, $n_2 = 12$, $p < 0.05$ two-tailed; Figure 5E). These findings suggest that $GABA_A$-mediated inhibition contributes to the suppression of fimbria-evoked EPSPs following the PFC train but does not account entirely for this suppression.

DISCUSSION

We found that high-frequency PFC stimulation suppresses EPSPs arising from single-pulse fimbria stimulation in VS MSNs. This suppression was observed at a short latency following the PFC stimulus (50 ms after the final pulse in a 10 pulse, 50 Hz train delivered to the PFC), but not at a long latency (500 ms) following the PFC train. The suppression of fimbria-evoked EPSPs by the PFC cannot be attributed solely to the depolarization of recorded cells elicited by the PFC train, as fimbria-evoked EPSPs were not attenuated by the depolarization elicited by spontaneous up states or current injection through the recording electrode. Moreover, burst-like activation of the PFC was necessary to produce suppression of fimbria responses; single-pulse stimulation of the PFC did not reduce the magnitude of the fimbria-evoked EPSP. The suppression of glutamatergic responses by robust PFC activation extended to other afferents as well, as PFC train stimulation attenuated thalamus-evoked responses. Trains of stimuli to the HP did not attenuate PFC-evoked EPSPs, consistent with the proposed gating relationship of the HP with VS MSNs (O'Donnell and Grace, 1995). However, burst-like stimulation of the thalamus was able to attenuate the PFC-evoked response, but this effect was not as dramatic as the near-total suppression of HP and thalamic inputs caused by PFC train stimuli. These data suggest that burst-like PFC activity elicits brief heterosynaptic suppression of HP and thalamic inputs to the VS.

The integration of excitatory inputs in the VS is complex, with several nonlinearities (Goto and O'Donnell, 2002; Wolf et al., 2009). HP afferents are critical for the spontaneous up states observed in anesthetized animals; VS up states are eliminated if the fimbria/fornix is transected or inactivated (O'Donnell and Grace, 1995) and can be detected simultaneously with HP spindles (Goto and O'Donnell, 2001b). As MSNs fire action potentials only from the up state, the relationship of the HP to the VS has been described as a gating mechanism, in which the VS must receive convergent excitatory input from the HP for other excitatory inputs, including those from the PFC, to be

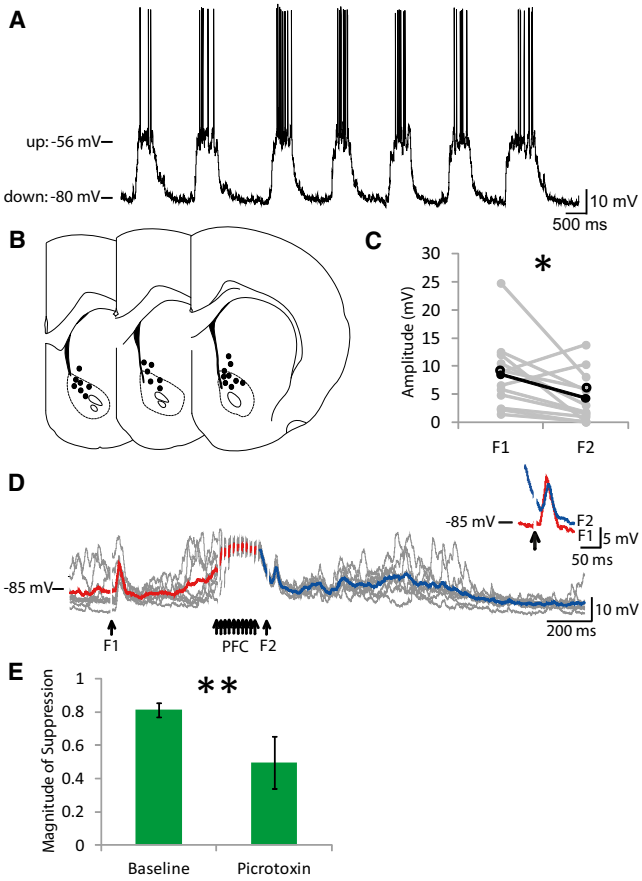

Figure 5. Picrotoxin Alleviates Some, but Not All, of the PFC-Mediated Suppression of EPSPs in VS MSNs

(A) Representative trace showing increased spontaneous firing in an MSN recorded with 200 μM picrotoxin in the intracellular solution. This cell transitioned to the up state at a frequency of 0.7 Hz and fired at 2.4 Hz.

(B) Illustration of recording sites in the VS using picrotoxin. Recorded cells fell within the same regions recorded without picrotoxin.

(C) Actual amplitude values of all F1 and F2 evoked responses recorded with picrotoxin in the intracellular solution (gray), and their average (closed black) indicating an overall suppression of F2 (*$p < 0.05$; paired t test). Open black circles indicate the example shown in (D).

(D) Overlay of responses to fimbria stimuli before and 50 ms following train PFC stimulation following picrotoxin treatment. Mean responses to F1 and F2 are highlighted in red and blue, respectively, and overlaid in the inset.

(E) Plot comparing the magnitude of suppression of the F2 response 50 ms following PFC train stimulation under baseline conditions and in the presence of picrotoxin. Picrotoxin reduced the magnitude of PFC-elicited suppression (**$p < 0.05$; two-tailed Mann-Whitney *U*). Error bars are mean ± SEM.

transmitted onward to downstream targets (O'Donnell and Grace, 1995). The critical role of the HP in shaping VS activity is also apparent in the behaving animal. Under resting conditions, the VS shows highly synchronous field potential activity with the ventral HP (Gruber et al., 2009a). Furthermore, place cells are found in the VS (Lavoie and Mizumori, 1994), and their activity is likely driven by HP inputs. These findings indicate that the HP gating of other inputs is a default mode of input integration by which contextual information is continuously updated in the VS.

Robust PFC Stimulation Evokes Heterosynaptic Suppression in the VS

The strong HP influence over VS activity is not insurmountable, however. During behavioral conditions that require PFC involvement, PFC pyramidal neurons fire in a brief burst-like pattern that can reach up to 30–50 Hz (Chafee and Goldman-Rakic, 1998; Peters et al., 2005), and cortical networks show high-frequency oscillations in that range (Sirota et al., 2008). Here, we found that PFC stimulus trains mimicking naturally occurring burst activity transiently suppress other inputs, including those arriving from the HP. In the behaving animal, decision-making epochs are marked by transient VS synchrony with the PFC. During these epochs, VS-HP coherence in the theta frequency band is reduced despite the persistence of strong theta activity in the HP (Gruber et al., 2009a). These data suggest that the PFC can commandeer control of VS activity during brief periods of high PFC activity. The fact that this transiently enhanced PFC-VS synchrony occurs in the face of unchanged HP activity suggests the interaction must take place within the VS. Here, we demonstrate that the PFC is capable of suppressing synaptic responses evoked by other inputs if, and only if, the PFC is strongly activated.

VS responses to HP and thalamic inputs are transiently suppressed by burst-like PFC activation in a manner that does not depend on depolarization. Although the PFC-evoked up state could attenuate HP and thalamic EPSPs by virtue of their occurring at a depolarized membrane potential, we found that the suppression persisted even if the post-PFC responses were compared to EPSPs recorded at the same membrane potential range. The experiments in which MSNs were artificially depolarized may be confounded by the limited space clamp of the recording configuration that limits the effective depolarization to very proximal sites; if the interactions that drive the observed suppression are more distal, somatic current injection is unlikely to affect the first EPSP. However, the cases in which the first HP- or thalamus-evoked EPSP was measured during spontaneous up states circumvent this confound, as up states are synaptically driven and also present in dendrites (Wolf et al., 2005). These data strongly argue for the absence of a membrane depolarization effect in the suppression we observed.

PFC train stimulation paradoxically evokes silent, activated states in VS MSNs. Despite producing a persistent depolarization in these neurons, trains of stimuli to the PFC do not result in action potential firing in the majority of the population (Gruber and O'Donnell, 2009). Here, burst PFC stimulation evoked action potentials in only 14.8% of recorded VS neurons under baseline conditions. This finding of limited MSN activation by PFC burst stimulation is comparable to the small percentage of MSNs showing c-*fos* activation by drug-associated cues in a learning paradigm (Koya et al., 2009). However, under experimental conditions in which $GABA_A$-receptor channels were blocked, PFC burst stimulation evoked action potential firing in a greater proportion of MSNs (50.0%). These data suggest that the lack of firing in normal conditions may be due to PFC recruitment of GABAergic processes. One interpretation of this set of findings is that the strong PFC activation required to guide goal-directed behaviors is likely encoded in a discrete distributed ensemble of VS neurons. For signals from the PFC to be

effectively relayed through sparse ensembles in the basal ganglia, it is essential to suppress irrelevant and competing neural activity. The heterosynaptic suppression elicited by PFC trains of action potentials may blunt excitatory activity in MSNs for a brief period following the PFC burst, allowing for the activation of spatially and temporally restricted sparse neural ensembles.

Several mechanisms are potentially responsible for the heterosynaptic suppression we observed in the VS. Activation of local fast-spiking GABAergic interneurons stands out as a strong possibility, as this cell population is highly activated by train PFC stimulation and produces feed-forward inhibition of PFC responses (Gruber and O'Donnell, 2009; Gruber et al., 2009b; Mallet et al., 2005; Taverna et al., 2007). We found that intra-MSN $GABA_A$ blockade reduced the extent of heterosynaptic suppression of HP inputs by PFC activation. This finding suggests that synaptic inhibition of MSNs contributes to the suppression of EPSPs following PFC train stimulation. As intracellular diffusion of PTX from high-resistance electrode tips may be limited to proximal sites, this manipulation is likely to underestimate the role of $GABA_A$ receptors. Although it is possible that recurrent inhibition of recorded neurons by neighboring MSN resulted in the observed suppression of responses, this alternative is unlikely because surround inhibition among striatal MSN is weak (Jaeger et al., 1994; Koos et al., 2004; Tunstall et al., 2002). Other potential mechanisms include molecules that can be produced postsynaptically and affect presynaptic terminals. In the VS, extensive data indicate endocannabinoids acting on CB1 receptors may reduce glutamate and GABA release (Lovinger and Mathur, 2012), possibly serving as mediators of heterosynaptic suppression. However, endocannabinoid action in this system also functions to suppress inhibitory input to MSNs (Adermark and Lovinger, 2007), which would at least partly oppose the effect reported here. A subset of VS MSNs contains dynorphin (Svingos et al., 1999), which upon release can act on presynaptic kappa receptors, reducing glutamate release (Hjelmstad and Fields, 2001, 2003). Understanding the role of these modulators in the complex integration of information within the VS will help us establish synaptic mechanisms underlying behavioral response selection, determine whether they are involved in neuropsychiatric conditions, and eventually provide clues as to novel therapeutic approaches.

Functional Consequences of PFC-Driven Heterosynaptic Suppression in the VS

Transient heterosynaptic suppression driven by strong PFC activity may facilitate transmission of PFC-related information by the VS through basal ganglia loops. Whereas HP inputs may subserve a critical gating function, the impact of burst-like PFC activity upon information processing in the VS is clearly distinct from that of HP activity. Behavioral studies indicate different functional impact of PFC and HP inputs to the VS. For example, whereas limbic afferents to the VS readily elicit self-stimulation behavior, similar PFC stimulation fails to do so (Stuber et al., 2011). More recently, optical stimulation of PFC afferents to the VS were found to be reinforcing in mice (Britt et al., 2012); however, in this case self-stimulation behavior required greater frequency and duration stimuli for PFC than HP or amygdala inputs to be effective. These findings suggest that cortical inputs may have a qualitatively different connectivity in VS circuits than HP inputs and that responses to convergent PFC and HP inputs may not be additive in the VS. We propose that suppression of HP responses by strong PFC activation may allow an efficient transfer of PFC commands through basal ganglia loops and an unhindered selection of the appropriate behavioral response.

As the role of thalamic inputs to the VS is not well understood, the functional implications of the PFC-thalamic input interaction are unclear. Thalamic afferents arriving to striatal regions primarily originate in the nonspecific nuclei (Groenewegen and Berendse, 1994). These projections are therefore likely to be involved in a global-activating function and perhaps in conveying crude sensory information. Transient suppression of this influence by strong PFC activation may facilitate the relay of PFC information through the VS with minimal disturbance from ongoing arousal state-related information.

The impact of bursts of PFC activity on VS physiology may be essential for supporting cognitive functions that depend on the PFC. The VS itself is critical for instrumental behavior and is required for the normal ability of animals to choose delayed reward (Cardinal et al., 2002). Furthermore, a distributed subset of VS neurons becomes active during decision points in a spatial navigation task (van der Meer and Redish, 2009). PFC-VS interactions are critical for rodent decision making (Christakou et al., 2004; St Onge et al., 2012) but are also important for human cognition. Deep electroencephalogram recordings during a reward-based learning task in humans reveal brief epochs of synchronous activity in the VS and medial PFC during decision-making instances (Cohen et al., 2009). In addition to transiently enhanced PFC-VS activity, several studies indicate that interactions between the HP and VS vary during epochs that require decisions. Simultaneous local field potential recordings from both structures reveal that ventral HP-VS coupling is altered during performance of a T-maze task (Tort et al., 2008) and in cue-guided lever pressing (Gruber et al., 2009a). Overall, these data illustrate that behavioral conditions that require decisions are characterized by enhanced PFC-VS coordination and varied HP-VS synchrony. The PFC-driven heterosynaptic suppression we report here may be responsible for the latter, thereby contributing to the VS output patterns that underpin executive functions.

Alterations to the PFC-VS projection have been implicated in neuropsychiatric disorders and addictive behaviors. For instance, synaptic responses and plasticity mechanisms in this pathway are affected in animals that self-administer cocaine (Lüscher and Malenka, 2011). An altered PFC-VS interaction that elicits inadequate heterosynaptic suppression of limbic inputs could result in the activation of inappropriate neural ensembles. This aberrant activation could thereby result in the inability to suppress behaviors, such as drug seeking. The nonlinear interactions among inputs to VS MSNs may be critical for shaping appropriate responses, and therefore strategies aimed at restoring these interactions may provide novel therapeutic approaches for disorders in which decision making is impaired.

EXPERIMENTAL PROCEDURES

Animal Subjects

Intracellular recordings from MSNs were obtained in vivo from 51 adult male Long Evans rats (310–460 g) purchased from Charles River Laboratories (Wilmington, MA, USA). All experiments were conducted in accordance with the United States National Research Council's *Guide for the Care and Use of Laboratory Animals* and were approved by the University of Maryland Institutional Animal Care and Use Committee.

Electrophysiological Recordings

In preparation for recording, rats were deeply anesthetized with chloral hydrate (400 mg/kg, intraperitoneally [i.p.]) and placed in a stereotaxic apparatus (David Kopf, Tujunga, CA, USA). Anesthesia was maintained throughout the duration of experiments by constant i.p. infusion of chloral hydrate (20–30 mg/kg/hr) via a minipump (Bioanalytical Systems, West Lafayette, IN, USA). Throughout recording experiments, rats were kept between 36°C and 38°C as measured by a rectal temperature probe (Fine Science Tools, Foster City, CA, USA). Bupivacaine (0.25%) was injected subcutaneously into the skin overlying the skull before a scalpel incision was made. Small burr holes were drilled into the skull to allow for electrode placement. A bipolar concentric stimulating electrode (outer diameter, 1 mm) with 0.5 mm of separation between the tips (Rhodes Medical Instruments, Woodland Hills, CA, USA) was placed into the right medial PFC (3.2 mm anterior to bregma, 2.0 mm lateral to midline, and 4.4 mm ventral to the pial surface) at a 30° angle toward midline. As a result of this protocol, the electrode entered the brain from the left of the midline and crossed into the right hemisphere with the tip terminating in the infralimbic/prelimbic region of the medial PFC. A second stimulating electrode was placed into the right fimbria (2.8 mm posterior to bregma, 3.8 mm lateral to midline, and 4.2 mm ventral to the pial surface). In a subset of animals (n = 14), the second stimulating electrode was placed into the right thalamus (2.8 mm posterior to bregma, 3.0 mm lateral to midline, and 4.2 mm ventral to the pial surface) instead of the fimbria. Current pulses through the stimulating electrodes were generated by ISO-Flex stimulus isolation units (AMPI, Jerusalem, Israel) driven by a Master 8 Stimulator (AMPI).

Intracellular microelectrodes were pulled from borosilicate glass tubing (1 mm outer diameter; World Precision Instruments, Sarasota, FL, USA) to a resistance of 40–110 MΩ using a P-97 Flaming-Brown microelectrode puller (Sutter Instruments, Novato, CA, USA). Recording electrodes were filled with 2% Neurobiotin (Vector Laboratories, Burlingame, CA, USA) in 2 M potassium acetate and lowered into the right limbic striatum (1.2–1.8 mm anterior to bregma, 1.2–1.4 mm lateral to midline, and 3.5–6.5 mm below the pial surface) using a model 2662 Direct Drive Micropositioner (David Kopf). In 15 animals, 200 μM picrotoxin (Sigma-Aldrich, St. Louis), the $GABA_A$ open-channel blocker, was included in the intracellular solution contained in the recording electrode. Electrical signals from impaled cell membranes passed through a chloride-coated silver wire housed inside the glass microelectrode via a headstage to an intracellular amplifier (IR-283, NeuroData, Delaware Water Gap, PA, USA). Intracellular signals were low-pass filtered at 2 kHz (FLA-01, Cygnus Technologies, Delaware Water Gap, PA, USA), digitized (Digidata 1322A, Axon Instruments, Union City, CA, USA), sampled at 10 kHz using Axoscope (Axon Instruments), and stored on a PC.

Stimulation Protocol

Once impaled, neurons were recorded in current-clamp mode at baseline for at least 5 min to ensure stability of membrane properties. Only cells exhibiting a resting membrane potential of at least −65 mV and action potential amplitude of at least 40 mV from threshold were used in this study. A series of positive and negative current steps delivered through the recording electrode (0.1–0.5 nA, 100 ms) were used to assess the input resistance of recorded cells. Subsequent to baseline recordings, the responses of stable cells to medial PFC and fimbria stimulation were assessed using the following protocol once every 15 s for 8–15 repetitions. A single-pulse stimulation of the fimbria (1.0 mA; 0.5 ms; F1) was delivered 500 ms before train stimulation of the mPFC (50 Hz train of ten pulses; 0.4–1.0 mA; 0.5 ms). A second fimbria pulse (1.0 mA; 0.5 ms; F2) was then delivered either 50 ms or 500 ms after the last pulse in the train stimulation of the PFC. This protocol was intended to test the effect of burst-like PFC stimulation on MSN responses to hippocampal inputs in the limbic striatum. An equivalent protocol (single-pulse stimulus to the thalamus, followed by a ten-pulse, 50 Hz train stimulation of the PFC at a 500 ms latency, followed by a second pulse to the thalamus at a 50 or 500 ms latency) was used in the animals receiving thalamic-stimulating electrode placement. The response of cells to fimbria or thalamus single-pulse stimulation 50 ms following single-pulse stimulation of the PFC was also considered in a subgroup of cells (n = 13). In some cases (n = 12), we injected depolarizing current through the recording electrode (between −0.2 and 0.2 nA) to record an F1 or T1 response during a depolarized membrane potential similar to that at which F2 and T2 responses were evoked. A subset of cells (n = 13) was also subjected to a stimulus protocol in which a single-pulse stimulus was delivered to the PFC (1.0 mA; 0.5 ms; PFC1), followed at a 500 ms latency by a train stimulation of the fimbria or thalamus (50 Hz train of ten pulses; 1.0 mA; 0.5 ms), after which a second pulse was delivered to the PFC (1.0 mA; 0.5 ms; PFC2). In all cases, responses to stimulation were averaged over all of the repetitions delivered to the cell.

Magnitude of Suppression Calculation

To calculate the magnitude of EPSP suppression, we first determined the ratio of the control and test pulses. For instance, in the cases in which we stimulated the fimbria, we calculated F2/F1 using response amplitudes. As this quotient represents the proportion of the response retained following PFC train stimulation, we expressed the difference between 1 and F2/F1 as a percentage to indicate the magnitude of EPSP suppression.

Histology

After baseline and stimulus-response recordings were collected, cells were filled with Neurobiotin by passing positive current (1 nA, 200 ms pulses, 2 Hz) for at least 10 min through the recording electrode. Upon completion of recording experiments, animals were euthanized with an overdose of sodium pentobarbital (100 mg/kg) and transcardially perfused with cold saline followed by 4% paraformaldehyde. Brains were then removed and postfixed in 4% paraformaldehyde for at least 24 hr before being transferred to a 30% sucrose solution in 0.1 M phosphate buffer. After at least 48 hr in sucrose, brains were cut into 50 μm sections using a freezing microtome and placed into phosphate buffer. Sections through PFC and fimbria or thalamus were mounted on gelatin-coated slides and Nissl stained to verify placement of stimulating electrodes. Sections through VS were processed for visualization of Neurobiotin-filled cells and then mounted on gelatin-coated slides and Nissl stained. All stained slides were coverslipped and examined microscopically for cell and electrode location.

ACKNOWLEDGMENTS

This work was supported by grants from the National Institutes of Health (R01 MH060131) to P.O.'D. and (R31 MH092043) to G.G.C.

Accepted: January 23, 2013
Published: April 10, 2013

REFERENCES

Adermark, L., and Lovinger, D.M. (2007). Retrograde endocannabinoid signaling at striatal synapses requires a regulated postsynaptic release step. Proc. Natl. Acad. Sci. USA *104*, 20564–20569.

Akaike, N., Hattori, K., Inomata, N., and Oomura, Y. (1985). gamma-Aminobutyric-acid- and pentobarbitone-gated chloride currents in internally perfused frog sensory neurones. J. Physiol. *360*, 367–386.

Alger, B.E., Megela, A.L., and Teyler, T.J. (1978). Transient heterosynaptic depression in the hippocampal slice. Brain Res. Bull. *3*, 181–184.

Berendse, H.W., and Groenewegen, H.J. (1990). Organization of the thalamostriatal projections in the rat, with special emphasis on the ventral striatum. J. Comp. Neurol. *299*, 187–228.

Brady, A.M., and O'Donnell, P. (2004). Dopaminergic modulation of prefrontal cortical input to nucleus accumbens neurons in vivo. J. Neurosci. *24*, 1040–1049.

Britt, J.P., Benaliouad, F., McDevitt, R.A., Stuber, G.D., Wise, R.A., and Bonci, A. (2012). Synaptic and behavioral profile of multiple glutamatergic inputs to the nucleus accumbens. Neuron *76*, 790–803.

Cardinal, R.N., Parkinson, J.A., Hall, J., and Everitt, B.J. (2002). Emotion and motivation: the role of the amygdala, ventral striatum, and prefrontal cortex. Neurosci. Biobehav. Rev. *26*, 321–352.

Chafee, M.V., and Goldman-Rakic, P.S. (1998). Matching patterns of activity in primate prefrontal area 8a and parietal area 7ip neurons during a spatial working memory task. J. Neurophysiol. *79*, 2919–2940.

Christakou, A., Robbins, T.W., and Everitt, B.J. (2004). Prefrontal cortical-ventral striatal interactions involved in affective modulation of attentional performance: implications for corticostriatal circuit function. J. Neurosci. *24*, 773–780.

Cohen, M.X., Axmacher, N., Lenartz, D., Elger, C.E., Sturm, V., and Schlaepfer, T.E. (2009). Neuroelectric signatures of reward learning and decision-making in the human nucleus accumbens. Neuropsychopharmacology *34*, 1649–1658.

Cupello, A., Palm, A., Rapallino, M.V., and Hydén, H. (1991). Can Cl^- ions be extruded from a gamma-aminobutyric (GABA)-acceptive nerve cell via GABAA receptors on the plasma membrane cytoplasmic side? Cell. Mol. Neurobiol. *11*, 333–346.

French, S.J., and Totterdell, S. (2002). Hippocampal and prefrontal cortical inputs monosynaptically converge with individual projection neurons of the nucleus accumbens. J. Comp. Neurol. *446*, 151–165.

French, S.J., and Totterdell, S. (2003). Individual nucleus accumbens-projection neurons receive both basolateral amygdala and ventral subicular afferents in rats. Neuroscience *119*, 19–31.

Fuentealba, P., Crochet, S., Timofeev, I., and Steriade, M. (2004). Synaptic interactions between thalamic and cortical inputs onto cortical neurons in vivo. J. Neurophysiol. *91*, 1990–1998.

Goto, Y., and O'Donnell, P. (2001a). Network synchrony in the nucleus accumbens in vivo. J. Neurosci. *21*, 4498–4504.

Goto, Y., and O'Donnell, P. (2001b). Synchronous activity in the hippocampus and nucleus accumbens in vivo. J. Neurosci. *21*, RC131.

Goto, Y., and O'Donnell, P. (2002). Timing-dependent limbic-motor synaptic integration in the nucleus accumbens. Proc. Natl. Acad. Sci. USA *99*, 13189–13193.

Groenewegen, H.J., and Berendse, H.W. (1994). The specificity of the 'nonspecific' midline and intralaminar thalamic nuclei. Trends Neurosci. *17*, 52–57.

Gruber, A.J., and O'Donnell, P. (2009). Bursting activation of prefrontal cortex drives sustained up states in nucleus accumbens spiny neurons in vivo. Synapse *63*, 173–180.

Gruber, A.J., Hussain, R.J., and O'Donnell, P. (2009a). The nucleus accumbens: a switchboard for goal-directed behaviors. PLoS ONE *4*, e5062.

Gruber, A.J., Powell, E.M., and O'Donnell, P. (2009b). Cortically activated interneurons shape spatial aspects of cortico-accumbens processing. J. Neurophysiol. *101*, 1876–1882.

Hjelmstad, G.O., and Fields, H.L. (2001). Kappa opioid receptor inhibition of glutamatergic transmission in the nucleus accumbens shell. J. Neurophysiol. *85*, 1153–1158.

Hjelmstad, G.O., and Fields, H.L. (2003). Kappa opioid receptor activation in the nucleus accumbens inhibits glutamate and GABA release through different mechanisms. J. Neurophysiol. *89*, 2389–2395.

Hoaglin, D., Mosteller, F., and Tukey, J. (1983). Understanding Robust and Exploratory Data Analysis (New York: Wiley).

Inomata, N., Tokutomi, N., Oyama, Y., and Akaike, N. (1988). Intracellular picrotoxin blocks pentobarbital-gated Cl^- conductance. Neurosci. Res. *6*, 72–75.

Jaeger, D., Kita, H., and Wilson, C.J. (1994). Surround inhibition among projection neurons is weak or nonexistent in the rat neostriatum. J. Neurophysiol. *72*, 2555–2558.

Koos, T., Tepper, J.M., and Wilson, C.J. (2004). Comparison of IPSCs evoked by spiny and fast-spiking neurons in the neostriatum. J. Neurosci. *24*, 7916–7922.

Koya, E., Golden, S.A., Harvey, B.K., Guez-Barber, D.H., Berkow, A., Simmons, D.E., Bossert, J.M., Nair, S.G., Uejima, J.L., Marin, M.T., et al. (2009). Targeted disruption of cocaine-activated nucleus accumbens neurons prevents context-specific sensitization. Nat. Neurosci. *12*, 1069–1073.

Lavoie, A.M., and Mizumori, S.J. (1994). Spatial, movement- and reward-sensitive discharge by medial ventral striatum neurons of rats. Brain Res. *638*, 157–168.

Lovinger, D.M., and Mathur, B.N. (2012). Endocannabinoids in striatal plasticity. Parkinsonism Relat. Disord. *18*(*Suppl 1*), S132–S134.

Lüscher, C., and Malenka, R.C. (2011). Drug-evoked synaptic plasticity in addiction: from molecular changes to circuit remodeling. Neuron *69*, 650–663.

Lynch, G.S., Dunwiddie, T., and Gribkoff, V. (1977). Heterosynaptic depression: a postsynaptic correlate of long-term potentiation. Nature *266*, 737–739.

Mallet, N., Le Moine, C., Charpier, S., and Gonon, F. (2005). Feedforward inhibition of projection neurons by fast-spiking GABA interneurons in the rat striatum in vivo. J. Neurosci. *25*, 3857–3869.

Meredith, G.E., Wouterlood, F.G., and Pattiselanno, A. (1990). Hippocampal fibers make synaptic contacts with glutamate decarboxylase-immunoreactive neurons in the rat nucleus accumbens. Brain Res. *513*, 329–334.

Metherate, R., and Ashe, J.H. (1993). Ionic flux contributions to neocortical slow waves and nucleus basalis-mediated activation: whole-cell recordings in vivo. J. Neurosci. *13*, 5312–5323.

Mogenson, G.J., Jones, D.L., and Yim, C.Y. (1980). From motivation to action: functional interface between the limbic system and the motor system. Prog. Neurobiol. *14*, 69–97.

Moss, J., and Bolam, J.P. (2008). A dopaminergic axon lattice in the striatum and its relationship with cortical and thalamic terminals. J. Neurosci. *28*, 11221–11230.

O'Donnell, P., and Grace, A.A. (1995). Synaptic interactions among excitatory afferents to nucleus accumbens neurons: hippocampal gating of prefrontal cortical input. J. Neurosci. *15*, 3622–3639.

Peters, Y.M., O'Donnell, P., and Carelli, R.M. (2005). Prefrontal cortical cell firing during maintenance, extinction, and reinstatement of goal-directed behavior for natural reward. Synapse *56*, 74–83.

Sirota, A., Montgomery, S., Fujisawa, S., Isomura, Y., Zugaro, M., and Buzsáki, G. (2008). Entrainment of neocortical neurons and gamma oscillations by the hippocampal theta rhythm. Neuron *60*, 683–697.

St Onge, J.R., Stopper, C.M., Zahm, D.S., and Floresco, S.B. (2012). Separate prefrontal-subcortical circuits mediate different components of risk-based decision making. J. Neurosci. *32*, 2886–2899.

Stuber, G.D., Sparta, D.R., Stamatakis, A.M., van Leeuwen, W.A., Hardjoprajitno, J.E., Cho, S., Tye, K.M., Kempadoo, K.A., Zhang, F., Deisseroth, K., and Bonci, A. (2011). Excitatory transmission from the amygdala to nucleus accumbens facilitates reward seeking. Nature *475*, 377–380.

Svingos, A.L., Colago, E.E., and Pickel, V.M. (1999). Cellular sites for dynorphin activation of kappa-opioid receptors in the rat nucleus accumbens shell. J. Neurosci. *19*, 1804–1813.

Taverna, S., Canciani, B., and Pennartz, C.M. (2007). Membrane properties and synaptic connectivity of fast-spiking interneurons in rat ventral striatum. Brain Res. *1152*, 49–56.

Tort, A.B., Kramer, M.A., Thorn, C., Gibson, D.J., Kubota, Y., Graybiel, A.M., and Kopell, N.J. (2008). Dynamic cross-frequency couplings of local field potential oscillations in rat striatum and hippocampus during performance of a T-maze task. Proc. Natl. Acad. Sci. USA *105*, 20517–20522.

Tunstall, M.J., Oorschot, D.E., Kean, A., and Wickens, J.R. (2002). Inhibitory interactions between spiny projection neurons in the rat striatum. J. Neurophysiol. *88*, 1263–1269.

van der Meer, M.A., and Redish, A.D. (2009). Covert expectation-of-reward in rat ventral striatum at decision points. Front. Integr. Neurosci. *3*, 1.

Voorn, P., Vanderschuren, L.J., Groenewegen, H.J., Robbins, T.W., and Pennartz, C.M. (2004). Putting a spin on the dorsal-ventral divide of the striatum. Trends Neurosci. *27*, 468–474.

Wolf, J.A., Finkel, L.H., and Contreras, D. (2009). Sublinear summation of afferent inputs to the nucleus accumbens in the awake rat. J. Physiol. *587*, 1695–1704.

Wolf, J.A., Moyer, J.T., Lazarewicz, M.T., Contreras, D., Benoit-Marand, M., O'Donnell, P., and Finkel, L.H. (2005). NMDA/AMPA ratio impacts state transitions and entrainment to oscillations in a computational model of the nucleus accumbens medium spiny projection neuron. J. Neurosci. *25*, 9080–9095.